Please input the preferred copyright option as mentioned in the attached "*SpaceOps-2023 Copyright Policy for Manuscripts and Presentations*"
e.g. "Copyright ©2023 by the Mohammed Bin Rashid Space Centre (MBRSC) on behalf of SpaceOps. All rights reserved."

SpaceOps-2023, ID # 226

Adaptive LQR Control of Space-Based Solar Power Systems Using Satellites Formation Flying

Thais Cardoso Franco[a]*, Caio Nahuel Sousa Fagonde[a], Willer Gomes dos Santos[a]

[a] Aeronautics Institute of Technology, Praça Marechal Eduardo Gomes, 50 - São José dos Campos/SP Brazil, thais.franco@ga.ita.br
* Corresponding Author

Abstract

Space-Based Solar Power (SBSP) has shown promise as a means of providing clean and renewable electrical energy as well as enabling distribution to resource-poor areas on Earth. The biggest advantage of the concept of collecting solar power in space and transmitting it to any location on Earth using microwaves is the ability to capture energy 24 hours a day regardless of seasonality without atmospheric losses, reducing the need for expensive solutions for energy storage. However, it is only feasible in terms of energy capture if the surface area of the solar panel exposed in space is too large. Extensive structures are expensive and unfeasible to be placed in orbit by current space launchers, as well, photovoltaic surfaces hinged in many parts increase complexity and risk of failure. As a solution, this work explores the control of Space-Based Solar Power using satellites in formation flying - several small satellites working together in a group to achieve the objective of a larger vehicle, where their dynamic states are coupled by a common control law. Despite many benefits, the use of formation flying is challenging in the matter of guaranteeing the desired attitude, the relative dynamics between the formation's satellites, and the correct orbital movement due to the existence of orbital perturbations. In this way, an in-depth study of control techniques is essential for mission performance. For this, the use of Adaptive controllers is promising: they are control systems that automatically adjust their parameters to compensate for changes in the process or environment. Consequently, they offer potential improvement when applied to complex systems, where the dynamics are poorly understood or change in a non-predictable way, providing systematic and flexible approaches to dealing with uncertainties, nonlinearities, and time-varying process parameters. Uncertainties, together with the need for high precision control, make adaptive controllers particularly attractive for formation flying. Since the satellites suffer deviations during the mission due to perturbations, the most significant perturbations are used in the simulations. Adaptive LQR (Linear–Quadratic Regulator) controllers proved to be efficient in controlling formations flying, specifically for Projected Circular Orbit (PCO) topologies. The precision obtained opens the possibility of generating future analyses with formations close to each other, which is excellent from the point of view of SBSP, as it allows for the positioning of more satellites in an area of the geostationary orbit, enabling fewer necessary launches.

Keywords: Space-Based Solar Power, Formation Flying, Adaptive LQR

1. Introduction

After falling by about 1% in 2020, due to the impacts of the Covid-19 pandemic, the global electricity demand grew by close to 5% in 2021 and 4% in 2022 driven by the global economic recovery. Renewables are expanding quickly but not enough to satisfy a strong rebound in global electricity demand, pushing CO2 emissions from the power sector again to record levels in 2022. Based on data from the International Energy Agency (IEA) [1], fossil fuel-based electricity generation was covered by 45% of additional demand in 2021 and 40% in 2022, with nuclear power accounting for the rest. As a result, carbon emissions from the electricity sector, which fell in both 2019 and 2020, increased by 3.5% in 2021, and increased again by 2.5% in 2022, which would take them to an all-time high. Electricity generation is the single largest source of energy-related CO2 emissions today, accounting for 36% of total energy-related emissions.

At this point, the International Energy Agency (IEA) advocates policies to establish the transformation of the electricity sector as central to achieving net-zero emissions in 2050 [1]. In the coming years, depending on favorable public policies and conditions of global financial institutions, the tendency is for important investments in renewable sources to boost the energy matrix for generating electricity. In this context, the Space-Based Solar Power (SBSP) system has shown promise for providing a future of clean and renewable electrical energy, as well as enabling distribution to resource-poor areas on Earth. The concept of collecting solar power in space and transmitting it to the Earth using microwaves was initially discussed in a science fiction magazine by Isaac Asimov [2] and it was first

Please input the preferred copyright option as mentioned in the attached "*SpaceOps-2023 Copyright Policy for Manuscripts and Presentations*"
e.g. "Copyright ©2023 by the Mohammed Bin Rashid Space Centre (MBRSC) on behalf of SpaceOps. All rights reserved."

proposed in a technical paper by P. E. Glaser in 1968 [3]. The biggest advantage of Space-Based Solar Power over ground installations is the ability to capture energy 24 hours a day regardless of seasonality, reducing the need for expensive solutions for energy storage. It can also be mentioned that solar energy collected in space does not present atmospheric losses and can be distributed to any location on Earth.

Two major problems need to be solved to make SBSP feasible. The first one is due to the development of the technology necessary for the transmission via microwaves of the energy absorbed by the space photovoltaic surfaces to the ground station [4]. The second issue, which will be discussed in this work, is that SBSP is only feasible in terms of energy capture if the surface area of the solar panel exposed in space is large. Extensive structures are expensive and unfeasible to be placed in orbit by current space launchers, as well, photovoltaic surfaces hinged in many parts increase complexity and risk of failure. As a solution, the use of formation flying of satellites in SBSP is studied in this paper. The approach is a trend toward new space missions in which several small satellites can work together in a group to achieve the objective of a larger monolithic vehicle. For that, their dynamic states are coupled by a common control law [5].

For this work, the considered topology, or configuration along with the orbital motion, is the Projected Circular Orbit (PCO) [5]. In such an approach, a leader spacecraft is controlled to a desired nominal orbit while the other vehicles, called followers, control their own states relative to the leader, creating a relative circular orbit around the leader satellite, when these are projected in the y-z plane of the local-vertical, local-horizontal reference frame (LVLH). In this way, this approach allows traditional periodic maneuvers to be performed by the leader for orbital correction, while the other satellites in the formation follow the natural dynamics of the leader's reference orbit to perform autonomous control and regulation of their relative states [5]. The proposed formation flying model considers that all satellites are at the same altitude and the minimum relative distance between the satellites is equivalent to the area of the solar panels.

Few studies currently exist on the use of formation flying for SBSP missions and mainly focused specifically on the evaluation of new control techniques. Takeichi, N. et al [6] first studied the concept of a solar power satellite system configured by formation flying. They described the solar power satellite system consists of two sunlight reflectors and an Earth-pointing segment in geostationary orbit. Zekavat, S. A. et al [7, 8] innovate studying a space-based solar power that uses networks of small LEO satellites and multiple power-collecting base stations implemented on the Earth to allow effective energy collection. Goh, S.T. et al [9] continue the study about a solar power harvesting technique that uses a network of LEO spacecraft formation flying, in which all spacecraft are orbiting in the same circular orbit, with a different initial true anomaly. In that paper, a frequency and phase angle synchronization method to cope with the Doppler effect is presented. Salazar, F. J. T. and Winter, O. C. [10] and Salazar, F. J. T. et al [11] present an SBSP system, consisting of a space mirror and a microwave energy generator-transmitter in formation. The formation flying motion is simulated by a linear approximation of the two-body problem, taking into account the effects of solar radiation pressure.

Goel, A. et al [12] describe a formation flying in a geostationary orbit, in which all the power can be transmitted instantaneously to a single receiving station on Earth, a project being developed by the California Institute of Technology (Caltech). The authors considered planar orbits in order to eliminate the possibility of modules shadowing each other. In the presence of disturbance due to solar radiation pressure, their paper considers that as the formation flying orbits the Earth, the orientation and position of each module have to be changed so as to optimize the angle made by the photovoltaic surface with respect to the Sun and by the antenna surface with respect to the receiving station on Earth. Finally, in [13], they continue the study and use sequential convex programming to optimize the dual goal of minimizing the propellant usage and maximizing the power delivered to the ground station.

In the concept of operating an SBSP mission in general, all satellites are equipped with an antenna transmitting electric energy pointing to Earth, so individually each of the satellites transmits the captured solar energy to the chosen ground station. It is also important to note that all satellites of this configuration are at the same nominal altitude and point their solar panels directly towards the Sun, i.e., the attitude of the modules varies depending on the positioning in orbit to ensure that the panels are positioned at right angles to the Sun and at the same time ensure the ideal positioning for antenna transmission. Despite many benefits, the use of this formation flying is challenging in the matter of guaranteeing the desired attitude, the relative dynamics between the formation's satellites, and the correct orbital movement due to the existence of orbital perturbations. In this way, an in-depth study of control techniques is essential for mission performance. And, for this approach, Adaptive controllers shows to be a promising study candidate.

Adaptive controllers are control systems that automatically adjust their parameters to compensate for changes in the process or environment [14]. Such a controller allows a real-time estimation of unknown parameters such as drag coefficient, thrust misalignment, magnitude error, satellite mass variation, and their inclusion in the control law.

Please input the preferred copyright option as mentioned in the attached "*SpaceOps-2023 Copyright Policy for Manuscripts and Presentations*"
e.g. "Copyright ©2023 by the Mohammed Bin Rashid Space Centre (MBRSC) on behalf of SpaceOps. All rights reserved."

Consequently, adaptive control systems offer potential improvement for complex process control, where the process is poorly understood or changes in a non-predictable way, providing systematic and flexible approaches to dealing with uncertainties, nonlinearities, and time-varying process parameters. Uncertainties, together with the need for high precision control, make adaptive controllers particularly attractive for satellite formation flying.

In this regard, this work proposes to evaluate the performance of a controller named Adaptive LQR described in [14] and apply it in an SBSP mission using satellites formation flying. This technique uses the standard infinite-time LQR control as the nominal controller but is integrated with an optimal adaptive controller based on online learning that takes into account the effects of neglected system dynamics and external disturbances. The standard LQR is a controller that has efficiency limitations when dealing with satellites formation flying over long distances due to nonlinear system dynamics becoming increasingly relevant, as is the case of this work. In this sense, the Adaptive LQR proves to be a promising alternative as shown in the literature, the authors demonstrate here that the controller performs much better than the nominal LQR controller and that it does not become efficient, rather it maintains its efficacy despite increasing eccentricity and baseline separation.

It was not found in the literature, any work that uses this type of controller applied in Space-Based Solar Power, establishing then as the main contribution of this work. In addition, orbital perturbations due to Earth's non-homogeneity and aerodynamic drag are considered in this analysis.

Section 2 presents the dynamics of the satellites and the considered orbital disturbances, while Section 3 describes the SBSP using the concept of formation flying. The Adaptive LQR controller is presented in Section 4, the results obtained in Section 5, and the conclusions in Section 6.

2. Satellite Dynamics

The two-body problem is an idealization of the orbit that allows an analytical solution to the equations of motion through the conic family (circle, ellipse, parabola, hyperbola) [15]. In this representation, only gravitational forces between two bodies are considered, which are treated as spheres of mass concentrated at their centers. The dynamics for a satellite on an orbital trajectory in the Earth-centered inertial frame (ECI) can be expressed by the following expression [14]:

$$\ddot{\boldsymbol{r}} + \frac{\mu \boldsymbol{r}}{r^3} = \ddot{\boldsymbol{a}}_{\boldsymbol{p}} \tag{1}$$

where, $\boldsymbol{r}$ is the position vector ($\boldsymbol{r} = [X, Y, Z]^T$), μ is the Earth's gravitational parameter, r is the absolute value of $\boldsymbol{r}$, i.e., $r = \left|\left|\boldsymbol{r}\right|\right| = \sqrt{X^2 + Y^2 + Z^2}$ and $\ddot{\boldsymbol{a}}_{\boldsymbol{p}}$ is the disturbing forces, which in the case of the two-body problem has zero value.

2.1 Orbital Disturbances

The movement of a satellite diverges from the Keplerian orbit, due to the fact that the satellite suffers the action of several external forces, altering its trajectory, also called perturbing forces. The solution to the problem considering the perturbations can be obtained using as a starting point the representation of the two-body problem (Eq. 1) and the perturbations can be added as additional forces, represented by $\ddot{\boldsymbol{a}}_{\boldsymbol{p}}$:

$$\ddot{\boldsymbol{a}}_{\boldsymbol{p}} = \ddot{\boldsymbol{r}}_{\boldsymbol{nHom}} + \ddot{\boldsymbol{r}}_{\boldsymbol{Drag}} \tag{2}$$

In this analysis, orbital disturbances are considered just due to the non-homogeneous distribution of the Earth's mass ($\ddot{\boldsymbol{r}}_{\boldsymbol{nHom}}$) and atmospheric drag ($\ddot{\boldsymbol{r}}_{\boldsymbol{Drag}}$).

2.1.1 Non-Homogeneity of the Earth

In a two-body problem, the Earth can be modeled as a mass concentrated in a single point, or as a homogeneous sphere. However, in reality, the Earth is an oblate body and its mass distribution is not homogeneous. For the orbital analysis, a correction factor, called the zonal harmonic coefficient, of degree 2, described by [16] was considered in the present study:

$$J_2 = 1082.63 \times 10^{-6}$$

Please input the preferred copyright option as mentioned in the attached "*SpaceOps-2023 Copyright Policy for Manuscripts and Presentations*"
e.g. "Copyright ©2023 by the Mohammed Bin Rashid Space Centre (MBRSC) on behalf of SpaceOps. All rights reserved."

This value of the zonal harmonic coefficient J_2 is obtained from satellite observations and appropriate measurements by the 1984 WGS (World Geodetic System) model [16]. In this way, the expression for $\ddot{\boldsymbol{r}}_{\boldsymbol{nHom}}$ can be written as:

$$\ddot{\boldsymbol{r}}_{\boldsymbol{nHom}} = \ddot{\boldsymbol{r}}_{J_2} \tag{3}$$

The expressions used for harmonic accelerations are described by [16]:

$$\ddot{\boldsymbol{r}}_{J_2} = -\frac{3}{2} J_2 \left(\frac{\mu}{r^2}\right)\left(\frac{R_e}{r}\right)^2 \begin{bmatrix} \left(1 - 5\left(\frac{Z}{r}\right)^2\right)\frac{X}{r} \\ \left(1 - 5\left(\frac{Z}{r}\right)^2\right)\frac{Y}{r} \\ \left(3 - 5\left(\frac{Z}{r}\right)^2\right)\frac{Z}{r} \end{bmatrix} \tag{4}$$

where R_e is the Earth's radius since the J_2 harmonic is the dominant harmonic; it generates a perceptible precession in the orbits of satellites close to Earth. This perturbation does not cause significant variations in the semi-major axis, inclination, and eccentricity; however, it generates quite significant variations in the right ascension of the ascending node, perigee argument, and mean anomaly [16].

2.1.2 Atmospheric Drag

Atmospheric drag is a predominant perturbation force in low altitude Earth orbits. The representation of the drag force on a satellite is the same as that of a vehicle in simplified atmospheric flight, derived from aerodynamic considerations [17]:

$$\ddot{\boldsymbol{r}}_{\boldsymbol{Drag}} = -\frac{1}{2}\rho\frac{C_d A}{m} v_{rel}{}^2 \frac{\boldsymbol{v_{rel}}}{||\boldsymbol{v_{rel}}||} \tag{5}$$

$$\boldsymbol{v_{rel}} = \boldsymbol{V} - \boldsymbol{\omega_{rot}} \times \boldsymbol{r} \tag{6}$$

where m is the mass of the satellite, A is the satellite's cross-sectional area, ρ is the atmospheric density varying with altitude calculated using the Jacchia Reference Atmosphere Model [18], C_d is the drag coefficient set to 2.2, $\boldsymbol{v_{rel}}$ is the satellite's velocity vector relative to the atmosphere, $\mathbf{V}$ is the satellite's velocity vector in the ECI system, $\boldsymbol{\omega_{rot}}$ is the Earth's rotation velocity vector, and ω_{rot} = 7.292115 × 10^5 rad/s is the Earth's rotation velocity modulus.

Aerodynamic drag reduces the orbital energy, causing secular decay in the semi-major axis, eccentricity, and perigee altitude. Since the satellite's velocity vector is located on the instantaneous orbital plane, the aerodynamic drag has no significant effect on the inclination and right ascension of the ascending node [19]. As a consequence of this effect, the satellite loses altitude, which can lead to its disintegration or re-entry due to atmospheric friction.

3. The Space-Based Solar Power using Satellite Formation Flying

According to NASA's Goddard Space Flight Center (GSFC), formation flying can be described as the process of tracking or maintaining the desired separation, orientation, or relative position between two or more satellites. At the expense of high complexity, coordinating smaller satellites has many benefits over single satellites, including simpler and more stable satellite designs [20], high-precision relative navigation [21], faster build times, more efficient fault detection [22], higher redundancy creation, optimization and trajectory control [23, 24], communication [25] and synchronization of attitudes [26, 27].

For any specific mission, the satellites relative configuration, also called topology, must be carefully chosen in order to mitigate natural perturbations and achieve the relative motion that is best suited for the mission's goals. The main ones portrayed in the literature are the String of Beads, the Non-coplanar, the Natural Motion Circumnavigation, and the Projected Circular Orbit, the latter used in this work [5]. In the process to obtain the optimal configuration of the formation flying for the space-based solar power system different topologies of the satellites need to be tested.

e.g. "Copyright ©2023 by the Mohammed Bin Rashid Space Centre (MBRSC) on behalf of SpaceOps. All rights reserved."

3.1 Projected Circular Orbit

To obtain a formation flying topology appropriate to the needs of this analysis, it is necessary to perform the design and evaluation of the orbits through the dynamics of the relative movement between, at least, two satellites. The Projected Circular Orbit (PCO) topology (Fig. 1) is a type of formation in which the follower satellites travel in a circular relative orbit around the leader satellite when projected in the horizontal y-z plane of the Local-Vertical, Local-Horizontal (LVLH) reference frame, where the x-axis is oriented along the radius vector, which is from the center of Earth to the center of this frame, the z-axis points in the direction along the orbital angular momentum vector which is perpendicular to the plane of the leader satellite orbit and, the y-axis completes the triad [6]. To build this formation, the geometric properties of Clohessy & Wiltshire equations (CW) are used, allowing them to be rewritten in the form of magnitude (ρ) and phase (α) [5]:

$$\begin{aligned} x(t) &= \rho_x \,\mathrm{sen}(n_0\, t + \alpha_x) \\ y(t) &= \rho_y + 2\rho_x \cos(n_0\, t + \alpha_x) \\ z(t) &= \rho_z \,\mathrm{sen}(n_0\, t + \alpha_z) \end{aligned} \tag{7}$$

where:

$$\begin{aligned} \rho_x &= \frac{\sqrt{\dot{x}^2(0) + x^2(0) n_0^2}}{n_0} \\ \rho_y &= y(0) - \frac{2\dot{x}^2(0)}{n_0} \\ \rho_z &= \frac{\sqrt{\dot{z}^2(0) + z^2(0) n_0^2}}{n_0} \\ \alpha_x &= \tan^{-1}\left(\frac{n_0 x(0)}{\dot{x}(0)}\right) \\ \alpha_z &= \tan^{-1}\left(\frac{n_0 z(0)}{\dot{z}(0)}\right) \end{aligned} \tag{8}$$

$x(0), y(0), z(0)$ are the initial relative position coordinates, $\dot{x}(0)$, $\dot{y}(0)$, $\dot{z}(0)$ are the initial relative velocity coordinates, and n_0=$\sqrt{\mu/a}$ is the satellite's mean motion, being a the major semiaxis.

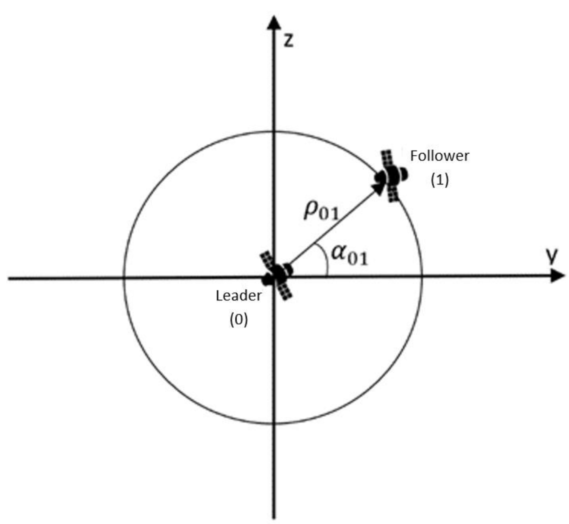

Please input the preferred copyright option as mentioned in the attached "*SpaceOps-2023 Copyright Policy for Manuscripts and Presentations*"
e.g. "Copyright ©2023 by the Mohammed Bin Rashid Space Centre (MBRSC) on behalf of SpaceOps. All rights reserved."

Fig. 1. Leader and follower vehicles layout.

Therefore, in order to have a projection on the y-z axis, which represents the PCO topology, the following considerations must be obeyed:

$$\alpha_x = \alpha_z \qquad \rho_x = \frac{\rho_z}{2} \tag{9}$$

The module of the relative distance between the leader and the follower is equal to:

$$\rho(t) = ||\rho(t)|| = \sqrt{x(t)^2 + y(t)^2 + z(t)^2} \tag{10}$$

However, in this work an analysis of the orbital dynamics will be conducted in the ECI frame, this practice will facilitate the addition of the terms referring to the orbital perturbations, since in the relative dynamics approach the deduction of the expressions for the orbital perturbations is more complex.

Based on these considerations, Fig. 2 presents the flowchart of conversion from relative to inertial dynamics, in which, at first, the dynamics of both the leader and the follower are converted to osculating elements to obtain the instantaneous vectors, later to mean elements, resulting in long-term evolution characteristics of the orbit. Finally, it is converted to the ECI and the orbital perturbations are added.

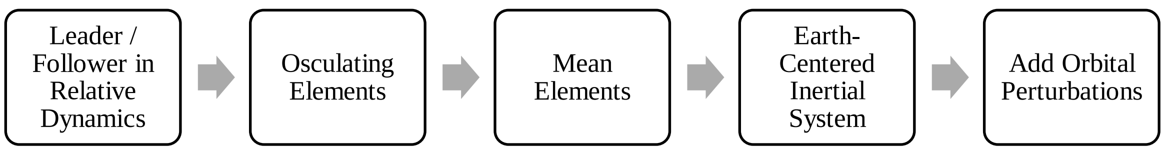

Fig. 2. Conversion from a relative dynamics system to an absolute dynamics system.

3.2 The Model: Distributed SBSP using Formation Flying

The formation flying model proposed as a Space-Based Solar Power is a collection of 16 satellites that fly close to each other in a geostationary orbit, being 4 leaders and 3 followers for each leader, i.e, four PCO with an inclination of 0°, 10°, 20° and 30°. Although not relevant to the analysis carried out in this work, the satellites could be considered as 16U CubeSats equipped with deployable solar panels. The solar panels are articulated and their plates overlap when they are closed, so that when open, they are similar to an umbrella over the satellite structure, justifying an area of Sun exposure of 10U², i.e., approximately 1m², as can be seen in Fig. 3a.

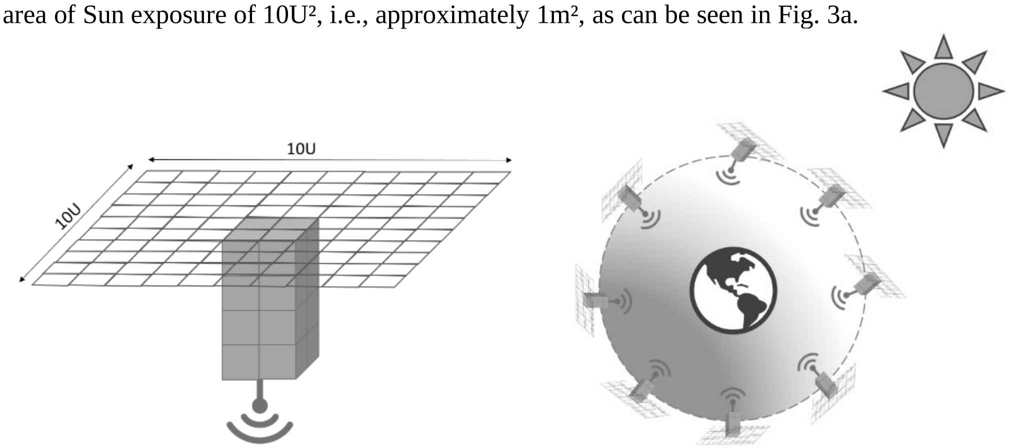

Fig. 3. (a) Each Distributed Formation Flying Module; (b) Changes in attitude towards the position of the Sun.

Although this work does not take into account the modeling of attitude, energy transmission between Sun-satellite-Earth, and electrical energy capture, it is important to bear in mind that all satellites of this configuration are at the same nominal altitude and point their solar panels directly towards the Sun, i.e., the attitude of the modules

e.g. "Copyright ©2023 by the Mohammed Bin Rashid Space Centre (MBRSC) on behalf of SpaceOps. All rights reserved."

varies depending on the positioning in orbit to ensure that the panels are positioned at right angles to the Sun and at the same time ensure the ideal positioning for antenna transmission as can be seen in figure Fig. 3b.

All satellites must acquire a ground station to transmit the captured solar energy by microwave. Both the ground station and the satellite have a transformer from solar to microwave energy and vice versa.

4. Adaptive LQR Control

Linear–quadratic regulator (LQR) is an optimal control technique which allows one to operate a given system at minimal cost based on a linear approximation of the system dynamics, given by the form [6]:

$$\dot{\boldsymbol{x}} = [A]\boldsymbol{x} + [B]\boldsymbol{u}\ . \tag{11}$$

Where $[A]$ and $[B]$ are matrices of appropriate dimensions and $\boldsymbol{x}$ is the state of the system.

The control law for $\boldsymbol{u}$ is obtained in this approach in Eq.11 by minimizing the following performance index [9]:

$$\mathcal{J} = 0.5 \int_0^{t_f} (\boldsymbol{x}^{\boldsymbol{T}}[Q]\boldsymbol{x} + \boldsymbol{x}^{\boldsymbol{T}}[R]\boldsymbol{x})\, dt \tag{12}$$

where t_f is the final time, and the matrices [Q] and [R] are parameters used to penalize each state or control action differently, thus determining the action of the controller. Both matrices are semi-definite positive and square.

For an autonomous system, constant weight matrices, and $t_f \rightarrow \infty$, the minimization of Eq. 12 is achieved by the following control law:

$$\boldsymbol{u} = -[K]\boldsymbol{x} \tag{13}$$

where $[K] = [R]^{-1}[B]^T[S]\boldsymbol{x}$ and [S] satisfies the Algebraic Riccati Equation [6]:

$$[S][A] + [A]^T[S] - [S][B][R]^{-1}[B]^T[S] + [Q] = 0 \tag{14}$$

whose solution is positive definite if the pair ($[A]$, $[B]$) is controllable and the pair ($[A]$, $[Q]^{0.5}$) is observable [12]. Positive definiteness of $[S]$ guarantees closed-loop stability, i.e., asymptotic stability of the system:

$$\dot{\boldsymbol{x}} = ([A]\ - [B][K])\boldsymbol{x}. \tag{15}$$

Hence the six-dimensional error vector, $\boldsymbol{e} = \boldsymbol{x} - \boldsymbol{x_r}$, satisfies:

$$\dot{\boldsymbol{e}} = [A]\boldsymbol{e}\ + [B]\begin{bmatrix} u_x - u_{xr} \\ u_y - u_{yr} \\ u_z - u_{zr} \end{bmatrix} \tag{16}$$

where,

$$[A] = \begin{bmatrix} 0 & 0 & 0 & 1 & 0 & 0 \\ 0 & 0 & 0 & 0 & 1 & 0 \\ 0 & 0 & 0 & 0 & 0 & 1 \\ 3\dot{\bar{M}}_0^{\ 2} & 0 & 0 & 0 & 2\dot{\bar{M}}_0 & 0 \\ 0 & 0 & 0 & -2\dot{\bar{M}}_0 & 0 & 0 \\ 0 & 0 & -\dot{\bar{M}}_0^{\ 2} - 2n_0\dot{\bar{\omega}}_0 & 0 & 0 & 0 \end{bmatrix} \tag{17}$$

$$[B] = \begin{bmatrix} 0_{3x3} \\ I_{3x3} \end{bmatrix} \tag{18}$$

and $\dot{\bar{M}}_0$ is the mean drift rate for the mean anomaly, and $\dot{\bar{\omega}}_0$ is the mean drift rate for the perigee argument.

e.g. "Copyright ©2023 by the Mohammed Bin Rashid Space Centre (MBRSC) on behalf of SpaceOps. All rights reserved."

However, the standard LQR is a controller that has efficiency limitations when dealing with satellites formation flying over long distances due to nonlinear system dynamics becoming increasingly relevant, as is the case of this work. In this sense, the Adaptive LQR proves to be a promising alternative as shown in the literature. In this way, the present work studies the Adaptive LQR controller proposed by Mathavaraj and Padhi [6] for formations flying dedicated to SBSP. In such a proposed controller, the standard infinite-time LQR is used as the nominal controller and augmented with neural networks that allow the control to capture the additional nonlinear and perturbative system effects. They also demonstrate that the controller performs much better than the nominal LQR controller and that it becomes efficient in systems with small eccentricities and large relative distances between satellites in formation flying operations.

In the process of learning function, the adaptive LQR method must also capture the non-modeled part of the system dynamics and, therefore it is based on the synthesis of two neural networks, called NN1 and NN2, whose weights are trained online. In this approach, one more term ($\boldsymbol{d(x)}$) is inserted in Eq. 19 responsible for the total uncertainty term in the system dynamics:

$$\dot{\boldsymbol{x}} = [A]\boldsymbol{x} + [B]\boldsymbol{u} + \boldsymbol{d}(\boldsymbol{x})\,. \tag{19}$$

Since it is desired that the states of the observer plant should track the states of the actual plant, the next key idea is to construct a "disturbance observer". The dynamics of which is represented using the subscript 0 as:

$$\dot{\boldsymbol{x}}_{\boldsymbol{0}} = [A]\boldsymbol{x} + [B]\boldsymbol{u} + \widehat{\boldsymbol{d}}(\boldsymbol{x}) + \boldsymbol{k}_{\boldsymbol{0}}(\boldsymbol{x} - \boldsymbol{x}_0) \tag{20}$$

where $\boldsymbol{k_0}$ is a positive definite gain matrix that needs to be selected by the designer for a good performance. And, it is necessary to simultaneously ensure $\boldsymbol{x} \to \boldsymbol{x}_0$ and $\boldsymbol{d}(\boldsymbol{x}) \to \widehat{\boldsymbol{d}}(\boldsymbol{x})$ as the plant starts operating, where $\widehat{\boldsymbol{d}}(\boldsymbol{x})$ is an approximation of the actual function $\boldsymbol{d}(\boldsymbol{x})$ after the transient process is over.

Since it is desired that the states of the observer plant should track the states of the actual plant, the error in state is:

$$\boldsymbol{e} = \boldsymbol{x} - \boldsymbol{x}_0 \tag{21}$$

The error in the dynamics can be obtained by differentiating Eq. 21 and then substituting in Eq. 20:

$$\dot{\boldsymbol{e}} = \dot{\boldsymbol{x}} - \dot{\boldsymbol{x}}_{\boldsymbol{0}} = \boldsymbol{d}(\boldsymbol{x}) - \widehat{\boldsymbol{d}}(\boldsymbol{x}) - \boldsymbol{k}_{\boldsymbol{0}} \tag{22}$$

In this way, $\widehat{\boldsymbol{d}}(\boldsymbol{x})$ is approximated as a linear-in-weight generic neural network $d_i(x)$ "time-varying" i, where W_i is the weight vector of the neural network and $\varphi_i(x)$ is the associated basis functions:

$$d_i(x) = {W_i}^T \varphi_i(x) \tag{23}$$

Neural network training NN2 is necessary as the true value of W_i. The NN2 neural network is trained following the procedure described in [6], generally using single-layer weighted linear networks based on radial basis functions, i.e., ways to approximate multivariable functions by using linear combinations of terms that are based on a single univariate function. For this, both the unmodeled part of the dynamics, crucial for online training, and its partial derivatives are captured. The weights use the per-channel error information in the state for training.

Usually using a radial basis function neural network, the neural network NN1 is trained in parallel, approximating the needed additional cost, based on the information provided by the online training algorithm NN2. The training of NN1 can also be seen in [6].

5. Results and Discussion

The analysis was simulated for a period of 7 and considering only 16 satellites: 4 PCO formations (S1, S2, S3 and S4) with 4 satellites each. Each formation is offset by 10° in inclination, i.e., inclinations ranging from 0, 10°, 20°, 30°, for S1 to S4, respectively. Each of the formations is composed of a leader satellite and three followers: follower 1 in a PCO with a radius of 250 km, follower 2 with a radius of 500 km and, follower 3 with a radius of 750

e.g. "Copyright ©2023 by the Mohammed Bin Rashid Space Centre (MBRSC) on behalf of SpaceOps. All rights reserved."

km. The first PCO in terms of the coordinates of relative positions can be seen in Fig. 4, where $e = 0$, $f = u = M$, $\omega = \Omega = 0°$ and a mean anomaly equal to zero ($M = 0°$).

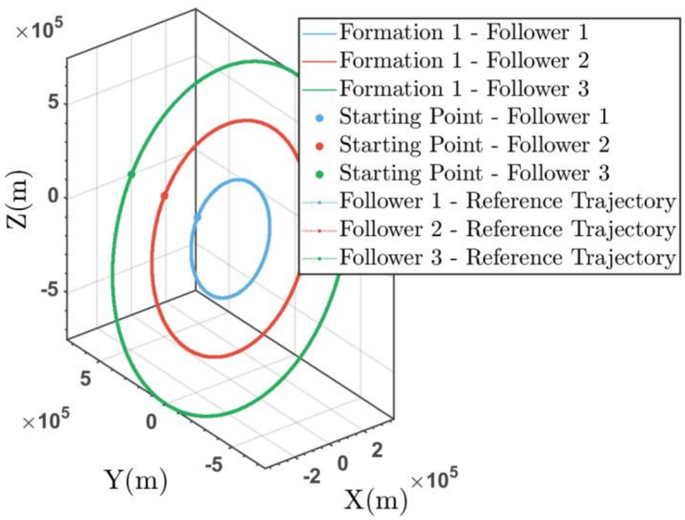

Fig. 4. Relative Orbit of the PCO Topology.

It is important to point out that the chosen distances, as well as the inclinations, are study parameters arbitrarily chosen in order to verify the performance of the Adaptive LQR controller and the obtained accuracy. Precision is of fundamental importance to verify the minimum possible distance between satellites that mitigates the possibility of collisions.

Fig. 5, shows the relative state of satellites as a function of time when the Adaptive LQR controller is activated in $t = 0$, i.e., the start of the simulation. The difference between the orbital relative position of the Follower 1 equivalent in each of the four formations flying can be verified in the coordinates X, Y, Z relative to formation number 1, that is, with zero inclination. Obviously, the difference of the Follower 1 of the first PCO relative to formation number 1 (itself) is zero, so it is not displayed.

In Fig. 6, it is possible to observe the position error of the Follower 1 of each of the four PCO formations in the coordinates X, Y, Z in relation to the leaders. The same procedure is repeated, then for Followers 2 (Fig. 7 and 8) and Followers 3 (Fig. 9 and 10).

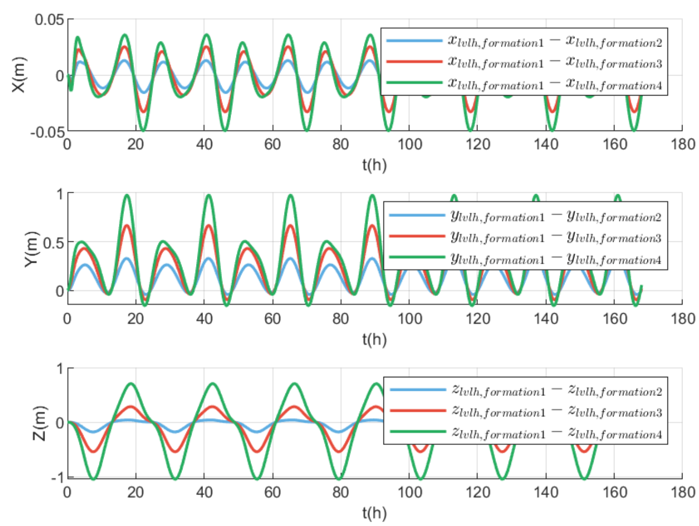

Fig. 5. Difference between the position (X, Y, Z) of Follower 1 of the four PCO relative to formation number 1.

Please input the preferred copyright option as mentioned in the attached "*SpaceOps-2023 Copyright Policy for Manuscripts and Presentations*"
e.g. "Copyright ©2023 by the Mohammed Bin Rashid Space Centre (MBRSC) on behalf of SpaceOps. All rights reserved."

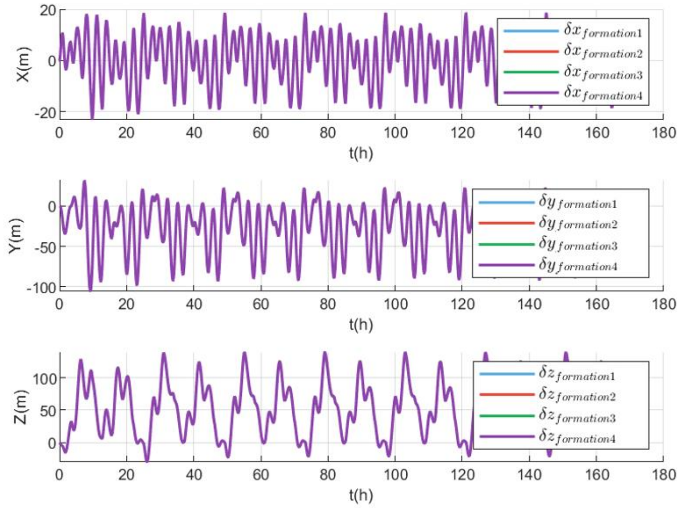

Fig. 6. Position error of the Follower 1 of each of the four PCO formations.

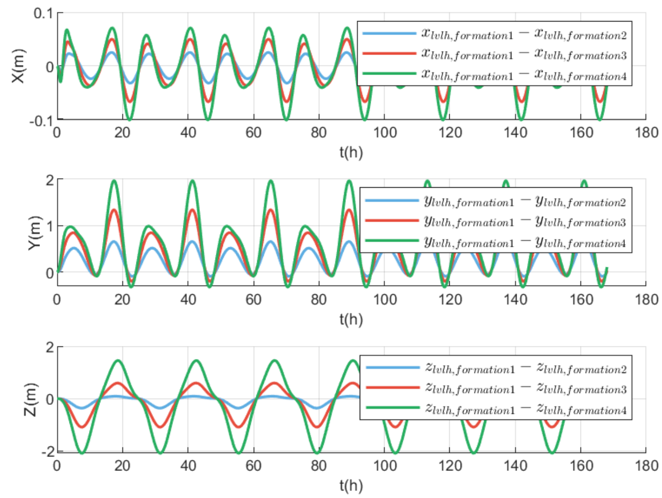

Fig. 7. Position of Follower 2 in the coordinates X, Y, Z.

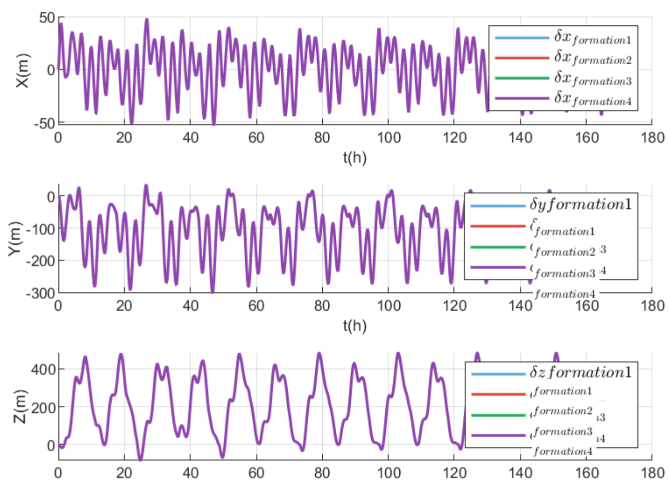

Fig. 8. Position error of the Follower 2 of each of the four PCO formations.

e.g. "Copyright ©2023 by the Mohammed Bin Rashid Space Centre (MBRSC) on behalf of SpaceOps. All rights reserved."

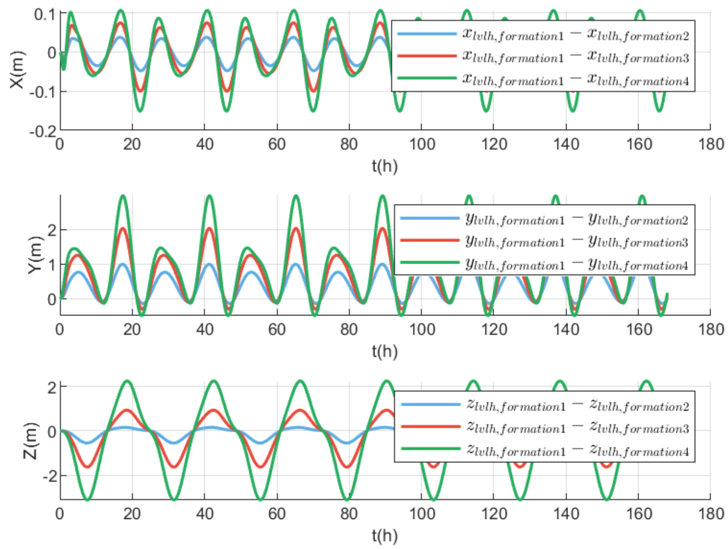

Fig. 9. Position of Follower 3 in the coordinates X, Y, Z.

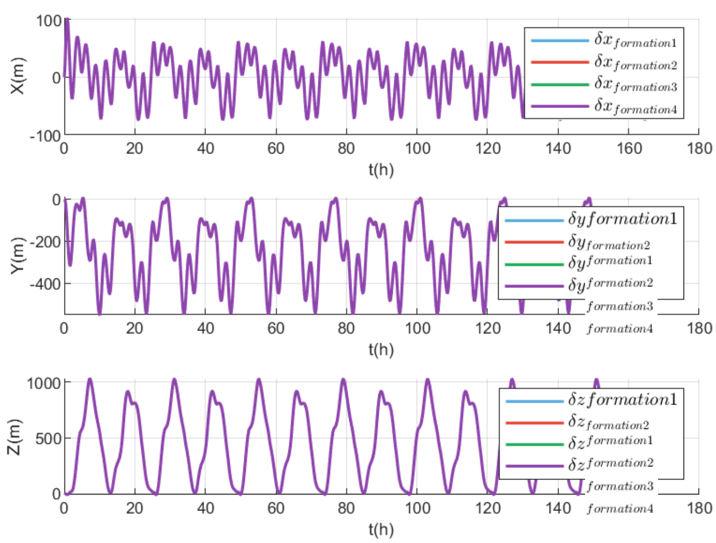

Fig. 10. Position error of the Follower 3 of each of the four PCO formations.

As it is possible to verify in Figs. 5, 7, and 9, during 7 days of simulation with the Adaptive LQR control engaged, greater variations occur the greater the inclination and the relative distance (radius) of the PCO in relation to the first formation.

Based on Figs. 6, 8, and 10, it was possible to maintain the formations with the controlled position in the three axes with an accuracy of 20 – 100 m in the X axis, approximately 100 – 500 meters in Y, and 150 – 1000 meters in the Z axis. This is due to the fact that the majority disturbance - the non-homogeneity modeled from harmonic J2 - causes oscillatory movements (Y and Z) and less significantly in the radial direction (X).

From the point of view of the feasibility of using the controller in relation to the positioning accuracy of the satellites, the graphs presented show promising results, which corroborates the progress in studies of this type of controller and opens up the possibility of generating new analyses that are more faithful to the SBSP project, i.e., with satellites flying closer to each other.

The analyses show that the higher the PCOs inclinations, the more negatively the controller performance is affected, causing greater ranges of positioning variations. The same occurs when comparing the performance of the

Please input the preferred copyright option as mentioned in the attached "*SpaceOps-2023 Copyright Policy for Manuscripts and Presentations*"
e.g. "Copyright ©2023 by the Mohammed Bin Rashid Space Centre (MBRSC) on behalf of SpaceOps. All rights reserved."

controller between followers 1 and 3. Variations in nominal relative positioning over time tend to be greater the greater the radius of the followers in relation to the leader.

6. Conclusions

Adaptive LQR controllers proved to be efficient in controlling formations flying, specifically for PCO topologies. The literature demonstrates that the nominal LQR does not perform well in formations with distant satellites [14], as was the case of the tested model, which demonstrates that the Adaptive LQR is a control approach to be considered and whose research should continue. However, despite the literature showing its superiority [14] and this work obtaining promising results, more tests are needed to compare its performance with the nominal LQR. The precision obtained opens the possibility of generating future analyses with formations close to each other, which is excellent from the point of view of SBSP, as it allows for the positioning of more satellites in an area of the geostationary orbit, enabling fewer necessary launches.

As future work, in addition to comparing controllers, we also want to estimate propellant consumption over time to assess feasibility from an operational point of view.

Acknowledgements

The authors would like to thank the Aeronautics Institute of Technology ("Instituto Tecnológico de Aeronáutica"-ITA) and the Coordination for the Improvement of Higher Education Personnel ("Coordenação de Aperfeiçoamento de Pessoal de Nível Superior" - CAPES), which financed part of this project (number 88887.512521/2020-00), as well as the E2MoC research group (CNPq certification number 466157) for their support.

References

[1] World Energy Outlook 2021, International Energy Agency (IEA), 2021. Online in: https://www.iea.org/reports/world-energy-outlook-2021

[2] I. Asimov, "Reason," I, Robot, 1941, pp. 59–77.

[3] P. E. Glaser, "Power from the sun: its future," Science, Vol. 162, No. 3856, 1968, pp. 857- 861.

[4] Costanzo Alessandra, Dionigi Marco, Masotti Diego, Mongiardo Mauro, Monti Giuseppina. Electromagnetic energy harvesting and wireless power transmission: A unified approach Proc. IEEE, 102 (11) (2014), pp. 1692-1712.

[5] K. T. Alfriend, S. R. Vadali, P. Gurfil, J. P. How, and L. S. Breger, Spacecraft Formation Flying, 1o Ed. Londres: Elsevier Ltd, 2010.

[6] N. Takeichi, H. Ueno, and M. Oda 2005 Feasibility Study of a Solar Power Satellite System Configured by Formation Flying, Acta Astronaut. 57 698-706.

[7] S. Zekavat, O. Abdelkhalik, S. Goh, and D. Fuhrmann, "A novel space-based solar power collection via leo satellite networks: Orbital management via wireless local positioning systems," in IEEE Aerospace Conference, Big Sky, MT, March 2010, pp. 1-9.

[8] S. Zekavat and O. Abdelkhalik, "Space-based power grids introduction: Feasibility study," in 2011 IEEE Aerospace Conference, Big Sky, MT, March 2011, pp. 1-6.

[9] S. T. Goh and S. A. Zekavat, "Space-based solar power via LEO satellite networks: Synchronization efficiency analysis," 2013 IEEE Aerospace Conference, Big Sky, MT, USA, 2013, pp. 1-9, doi: 10.1109/AERO.2013.6497319.

[10] Salazar F J T, McInnes C R and Winter O C 2016 Periodic orbits for space-based reflectors in the circular restricted three-body problem, Celest. Mech. Dyn. Astron. doi:10.1007/s10569-016-9739-3

[11] Salazar F J T, McInnes C R and Winter O C 2017 Solar Power Satellite system in formation on a common geostationary orbit. J. Phys.: Conf. Ser. 911 012006. doi: 0.1088/1742-6596/911/1/012006

Please input the preferred copyright option as mentioned in the attached "*SpaceOps-2023 Copyright Policy for Manuscripts and Presentations*"
e.g. "Copyright ©2023 by the Mohammed Bin Rashid Space Centre (MBRSC) on behalf of SpaceOps. All rights reserved."

[12] A. Goel, N. Lee and S. Pellegrino, "Trajectory design of formation flying constellation for space-based solar power," 2017 IEEE Aerospace Conference, Big Sky, MT, USA, 2017, pp. 1-11, doi: 10.1109/AERO.2017.7943711.

[13] Goel, Ashish and Chung, Soon-Jo and Pellegrino, Sergio (2017) Trajectory Design of a Spacecraft Formation for Space-Based Solar Power Using Sequential Convex Programming. In: Proceedings 9th International Workshop on Satellite Constellations and Formation Flying, Art. No. 17-43.

[14] S. Mathavaraj and R. Padhi. Satellite Formation Flying. High Precision Guidance using Optimal and Adaptive Control Techniques; Springer Nature: Singapore, 2021.

[15] Marcel J. Sidi. Spacecraft Dynamics and Control: A Practical Engineering Approach. Cambridge University Press, Cambridge, 1997.

[16] V. A. Chobotov, "Orbital mechanics", third edition, Jan 2002. [Online]. Available: http://dx.doi.org/10.2514/4.862250.

[17] C.-C. G. Chao, Applied Orbit Perturbation and Maintenance. Washington, DC: American Institute of Aeronautics and Astronautics, Inc., 2005.

[18] CCMC, "Standard Jacchia Reference Atmosphere 1977." https://ccmc.gsfc.nasa.gov/modelweb/atmos/jacchia.html.

[19] Byron D. Tapley, Bob E. Schutz and George H. Born. Statistical Orbit Determination. Elsevier Academic Press.

[20] C. W. T. Roscoe, J. J. Westphal, J. D. Griesbach and H. Schaub, "Formation establishment and reconfiguration using differential elements in J2-perturbed orbits," 2014 IEEE Aerospace Conference, Big Sky, MT, USA, 2014, pp. 1-19, doi: 10.1109/AERO.2014.6836272.

[21] O. Montenbruck, M. Wermuth, R. Kahle (2011) GPS based relative navigation for the TanDEM-X mission—first flight results. Navigation 58(4):293–304. doi:10.1002/j.2161-4296.2011.tb02587.x

[22] D. Lee, KD. Kumar, M. Sinha (2014) Fault detection and recovery of spacecraft formation flying using nonlinear observer and reconfigurable controller. Acta Astronaut 97:58–72. doi:10.1016/j.actaastro.2013.12.002

[23] B. Wu, D. Wang, EK. Poh, G. Xu (2009) Nonlinear optimization of low-thrust trajectory for satellite formation: legendre pseudospectral approach. J Guid Control Dyn 32(4):1371–1381. doi:10.2514/1.37675

[24] B. Wu, G. Xu, X. Cao (2016) Relative dynamics and control for satellite formation: accommodating J2 perturbation. J Aerosp Eng 4016011. doi:10.1061/(ASCE)AS.1943-5525.0000600

[25] Roy S. Smith and Fred Y. Hadaegh. Closed-loop dynamics of cooperative vehicle formations with parallel estimators and communication. IEEE Transactions on Automatic Control,52(8):1404–1414, 2007.

[26] B. Wu, D. Wang, EK. Poh (2011) Decentralized robust adaptive control for attitude synchronization under directed communication topology. J Guid Control Dyn 34(4):1276–1282. doi:10.2514/1.50189

[27] B. Wu, D. Wang, EK. Poh (2013) Decentralized sliding-mode control for attitude synchronization in spacecraft formation. Int J Robust Nonlinear Control 23(11):1183–1197. doi:10.1002/rnc.2812